Z. Phys. A - Atoms and Nuclei 304, 167-175 (1982)

Zeitschrift für Physik A Atoms and Nuclei

Vibrational Predissociation of SF_6 Dimers and Trimers

J. Geraedts, S. Stolte, and J. Reuss
Fysisch Laboratorium, Katholieke Universiteit, Nijmegen, The Netherlands

Received September 8, 1981

IR photo-dissociation spectra of SF_6 clusters have been studied. A He-seeded molecular beam has been attenuated by crossing it with a line tunable cw CO_2 laser of moderate power. - In the electron bombardment beam ionizer ($E_{el}=100\,eV$) small neutral clusters are found to fragment predominantly to the main monomer mass (SF_5^+). - Predissociation spectra have been calculated for clusters containing up to six SF_6-molecules invoking the dipole-dipole resonance force to lift the degeneracy of the molecule - excited molecule interaction. On the basis of these spectra, dimer and trimer concentrations have been determined quantitatively, for different molecular beam conditions.

1. Introduction

Recently we have shown [1] that predissociation of $(SF_6)_2$ leads to a simple double-peaked absorption spectrum, with a spacing of $20\,cm^{-1}$ and a linewidth of about $3\,cm^{-1}$ fwhm. By measuring the attenuation of an SF_6 molecular beam on axis caused by a line tunable cw CO_2 laser of moderate power, one obtains the absorption-spectrum. The typical attenuation peaks - at $935\,cm^{-1}$ and $955\,cm^{-1}$ - allowed us to single out the neutral parent-dimers in the molecular beam and to observe their fragmentation in the mass-spectrometer ionizer.

For higher stagnation pressures larger cluster fragment ions become detectable; we have also analyzed the attenuation spectra under these conditions. Although no unambiguous correspondence has been found between the sharp spectral features and the single parent clusters, a fit of a theoretical cluster spectrum to the measured attenuation curves yields the neutral cluster concentrations. All present measurements have utilized an electron bombardment ionizer for mass spectrometric detection with an electron energy of 100 eV, leading to high fragmentation probabilities of the clusters upon ionization. Correspondingly we detect the attenuation of the SF_5^+-ion signal as consequence of the interaction of the CO_2 laser photons with the molecular beam, because the strong fragmentation of small clusters results in highest detectibility of these clusters on mass SF_5^+.

In the analysis a simple interaction potential of the electric dipole-dipole type (R^{-3}) suffices to describe the observations. This dominant resonant force has been discussed by many authors at great lengths, e.g. Mullikan [2], Hirschfelder [3] and Margenau [4]. To our knowledge the two sharp dimer-peaks of the attenuation spectrum are the first direct measurements of resonant dipole-dipole forces between molecules. Of the two interacting molecules one is in the vibrational ground state and the other one is excited in the ν_3-mode. The molecule SF_6 is especially suitable to reveal this interaction because in the threefold degenerate ν_3-mode the molecule behaves like an isotropic harmonic oscillator, in good approximation. Perturbations, e.g. Coriolis forces cause effects which are much smaller than the observed splitting of $20\,cm^{-1}$. The large dipole transition matrix element μ_{01} of the ν_3-mode of SF_6 (0.388 D [5]) is responsible for the large splitting observed.

To produce clusters we have used beams of pure SF_6 and of 5% SF_6-He and 5% SF_6-Ar mixtures. On the masses of He^+ and Ar^+ we also have detected a weak laser-induced attenuation signal. This indicates that there are neutral $(SF_6)_n-(He)_m$ and $(SF_6)_n-(Ar)_m$ complexes present in the beam.

0340-2193/82/0304/0167/$01.80

Their concentration is too weak to influence the present spectra.

In this paper we restrict ourselves to the observations made with the 5% SF_6 – He mixture. The source conditions are characterized by a stagnation temperature $T_0 = 233$ K, a stagnation pressure P_0 between 1,000 and 1,850 torr and a nozzle diameter of 30 μm; only casual remarks will be found based on observations at other source conditions.

The SF_6-component consist of 4.2% $^{34}SF_6$-molecules [8]. The dimers will therefore include 8% $^{34}SF_6 \cdot {}^{32}SF_6$-complexes. The measured spectra contain one distinct attenuation peak of this mixed dimer at 921 cm^{-1}. Other peaks were not yet observed.

Recently, the predissociation lifetime of the vibrationally excited N_2O dimer was calculated [6] and compared with the limiting values of 10^{-4}–10^{-7} s, obtained experimentally [7]. In order to find agreement Morales and Ewing had to invoke a resonant dipole-dipole force. The results of the present paper on $(SF_6)_n$ may be regarded as strong backing of their argumentation.

2. The Experiment

The apparatus is shown schematically in Fig. 1. The molecular-beam machine consists of five separate vacuum chambers, each with its own pumping system. In the source chamber the beam is produced by gas expansion through a nozzle of 30 μm [9]. After a distance of 10–15 mm the beam passes through a skimmer (sk 1) into the buffer chamber. In the next chamber the chopper (ch 1) and the velocity selector

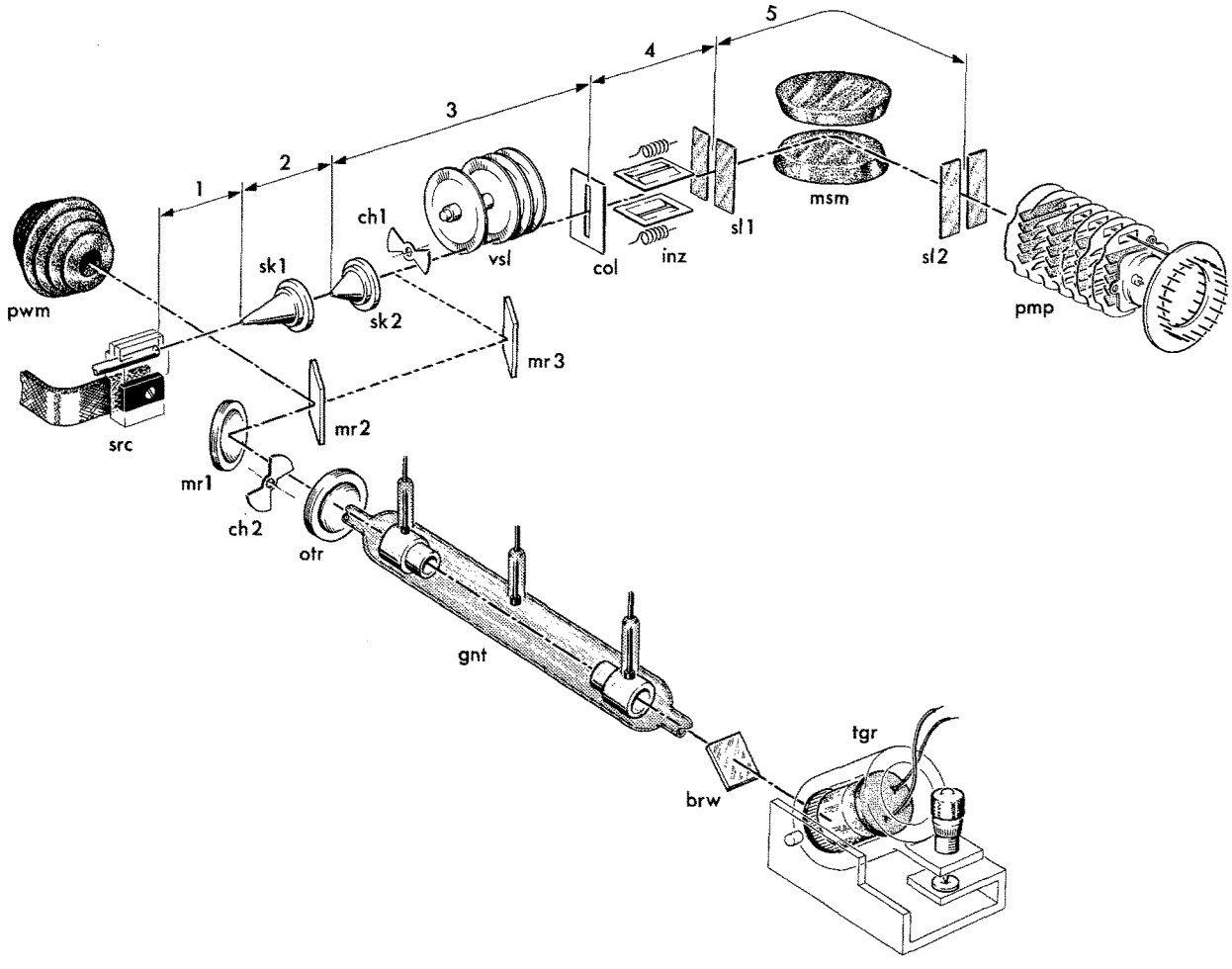

Fig. 1. The experimental set up. The molecular beam apparatus consists of the source (src, 0.03 mm ∅), skimmer 1 (sk 1, 1.1 mm ∅), skimmer 2 (sk 2, 3 mm ∅), the chopper (ch 1). the velocity selector (vsl), the collimator (col, 1.3 * 1.8 mm^2), the ionizer (inz), slit 1 (sl 1, 1.3 mm), the mass spectrometer magnet (msm), slit 2 (sl 2, 1.3 mm) and the particle multiplier (pmp). The laser system consists of the tunable grating (tgr), the brewster angle window (brw), the gain tube (gnt), the plano concave output reflector (otr), the chopper (ch 2), the concave mirror (mr 1), and one flat mirror (mr 2 or mr 3), and the power meter (pwm). The distances are 10 mm (1), 300 mm (2), 1500 mm (3), 900 mm (4) and 1500 mm (5)

(vs *l*) - slotted disk type - are mounted. In the fourth chamber the molecular beam is ionized by means of a high efficiency ionizer (inz) and, in the fifth chamber, focussed by ion lenses into the mass spectrometer magnet (msm) - 14 mm pole diameter, 0-9 kGauss - to be detected by a particle multiplier (pmp) at the end of the machine. The maximum pressures - under working conditions - are: 10^{-3} torr (1); $5\cdot10^{-6}$ torr (2); $5\cdot10^{-7}$ torr (3); $<10^{-8}$ torr (4) and $5\cdot10^{-7}$ torr (5).

The lasersystem consist of a line tunable cw CO_2 laser [10], a chopper (ch 2), a power meter (pwm) and a spectrum analyzer. The laser has a flow system and operates typically at a total pressure of 30 torr. The gas flows through a longitudinally excited gain tube (gnt). The maximum single-line power ranges from 5 W to 45 W and is found to be stable within 2% over several hours.

Two choppers - one in the molecular-beam (ch1) machine and one in the laser-system (ch 2) - permit phase - sensitive detection, either of the molecular beam or of the effect of the laser radiation on the molecular beam.

The experimental data, the molecular beam signal and the laser power, are directly transferred to an AIM-65 microcomputer (Rockwell Corp.) for storage and data reduction. The microcomputer also monitors the temperature of the source and the flux in the m.s. magnet.

The laser beam crosses the molecular beam at a right angle, between nozzle (30 μm ∅) and skimmer (1.1 mm ∅), about 7 mm downstream the nozzle. The position of this intersection has been changed with respect to [1]. Another change is that for the present results the laser has been focussed to a two times smaller waist. The spectra discussed in Sect. 4 are measured at 1 Watt laser power. Changing the laser frequency the power level was adjusted by changing the discharge current in the gain tube of the laser. Power reduction was achieved by utilizing a wire mesh (stainless steel, 0.2 mm ∅, $0.5*0.5\,mm^2$ opening). With a molecular beam velocity of about 870 m/s and the assumption of a Gaussian laser beam profile with a wast of 0.7 mm, 1 W corresponds with a laser fluency of $1.3\,J/m^2$.

The molecular beam collimation is effected by the skimmer (sk 1) and a collimator (col). Fragments with a transverse recoil velocity $\geqq 30$ m/s do not pass through this slit (col). No effect of monomer recoil (i.e. beam attenuation) is detectable [1].

3. Theoretical Spectrum

We assume that the geometry of a SF_6-cluster agrees with the equilibrium-geometry of clusters as calculated by Bonisent and Mutaftschiev [11]. In Table 1 we give the positions $\mathbf{R}_i$ for $1\leqq i\leqq 6$ of the SF_6-molecules in a hexamer which is fixed in x, y, z-space. The oligomers up to and including the hexamer, $n=6$, are built up by adding each time one SF_6-molecule to the previous structure, starting from the monomer, $n=1$. The length of the distance vector $\mathbf{R}_{ij}=\mathbf{R}_i-\mathbf{R}_j$ between two nearest neighbour molecules i and j for $1\leqq i\neq j\leqq n$ in a cluster is determined by the isotropic SF_6-SF_6-interaction. In Table 1 this distance is taken unity. An SF_6 molecule behaves as a three-dimensional oscillator and has three orthogonal equivalent vibrational axes, $\mathbf{x}_i$, $\mathbf{y}_i$ and $\mathbf{z}_i$ what concerns the ν_3-mode.

Table 1. The components of the position vectors $\mathbf{R}_i=(x_i, y_i, z_i)$ for clusters containing up to six SF_6-molecules. Nearest neighbours distances are unity

i	1	2	3	4	5	6
x_i	$-\sqrt{3}/3$	$\sqrt{3}/6$	$\sqrt{3}/6$	0	0	$5\sqrt{3}/9$
y_i	0	1/2	−1/2	0	0	0
z_i	0	0	0	$\sqrt{6}/3$	$-\sqrt{6}/3$	$2\sqrt{6}/9$

In good approximation the observed spectral features correspond to the eigen values of an interaction hamiltonian which contains as operator solely dipole-dipole terms

$$H_{DD}=\frac{1}{4\pi\varepsilon_0}\sum_{i<j}R_{ij}^{-3}\cdot[\boldsymbol{\mu}_i\cdot\boldsymbol{\mu}_j-3(\boldsymbol{\mu}_i\cdot\hat{\mathbf{R}}_{ij})(\boldsymbol{\mu}_j\cdot\hat{\mathbf{R}}_{ij})] \quad (3.1)$$

where $R_{ij}=|\mathbf{R}_{ij}|$, $\hat{\mathbf{R}}_{ij}=\mathbf{R}_{ij}/R_{ij}$ and where $\boldsymbol{\mu}_i$ represents the dipole operator.

The total wave functions of a simply excited cluster can be written as, e.g.

$$|x_1, y_1, z_1, --, x_i, y_i, z_i^\dagger, --, x_n, y_n, z_n\rangle=|z_i^\dagger\rangle \quad (3.2)$$

indicating that only one molecule i is excited and the excitation is along the z-axis. The $3n$ wave functions form a subset of degenerate states if H_{DD} is neglected.

Only the matrix elements between different singly excited eigen functions are non-vanishing, e.g.

$$\langle x_i^\dagger|H_{DD}|y_j^\dagger\rangle\neq 0, \quad \text{if } i\neq j \quad (3.3)$$

Diagonalization of the energy-matrix for a n-cluster yields the eigen values, i.e. the energy shifts $\Delta_{n,m}$ with respect to the fundamental frequency. The eigen functions $|u_{n,m}\rangle$ are used to calculate the transition strengths

$$S_{n,m}\propto|\langle u_{n,m}|\boldsymbol{\mu}|0\rangle|^2 \quad (3.4)$$

where $|0\rangle$ indicates the groundstate $|x_1, y_1, --, z_n\rangle$ and $\boldsymbol{\mu}=\sum_{i=1}^{n}\boldsymbol{\mu}_i$.

Table 2. The theoretical spectrum. The energy shift $\Delta_{n,m}$ is in units of $(4\pi\varepsilon_0)^{-1}\cdot\mu_{01}^2\cdot\langle R^{-3}\rangle$, where R describes the nearest neighbour distance and $\mu_{01}=0.388D$. The column $g_{n,m}$ describes the degeneracy and $g_{n,m}\cdot S_{n,m}$ the total transition strength – from the ground state to a individual excited level m – of an n-cluster

m	$\Delta_{n,m}$	$g_{n,m}$	$g_{n,m}\cdot S_{n,m}$
monomer, $n=1$			
1	+0.00	3	3.00
dimer, $n=2$			
1	−2.00	1	2.00
2	−1.00	2	0
3	+1.00	2	4.00
4	+2.00	1	0
trimer, $n=3$			
1	−2.50	1	0
2	−1.93	2	4.34
3	−1.00	2	0
4	+1.43	2	1.66
5	+2.00	1	3.00
6	+3.50	1	0
tetramer, $n=4$			
1	−2.50	3	0
2	−1.89	3	6.70
3	+0.50	2	0
4	+2.39	3	5.30
5	+5.00	1	0
pentamer, $n=5$			
1	−3.09	2	0
2	−2.50	1	0
3	−2.04	2	2.66
4	−1.97	1	4.46
5	−1.80	1	0
6	−0.86	2	1.99
7	+1.86	2	0
8	+2.63	2	5.35
9	+3.51	1	0.54
10	+5.76	1	0
hexamer, $n=6$			
1	−3.34	1	0
2	−3.32	1	0.0015
3	−2.88	1	0.011
4	−2.56	1	0.38
5	−2.21	1	4.13
6	−2.12	1	1.07
7	−1.90	1	0.44
8	−1.57	1	0.94
9	−1.47	1	0
10	−1.36	1	2.70
11	+0.54	1	1.06
12	+0.59	1	1.60
13	+2.54	1	0.10
14	+2.61	1	0
15	+2.63	1	3.31
16	+3.36	1	1.87
17	+4.24	1	0.38
18	+6.25	1	0.00014

Table 3. Energy shifts and transition probabilities for the mixed-dimer $^{34}SF_6\cdot{}^{32}SF_6$. The index m describes a particular transition, $\Delta_{2,m}$ the energy shift in cm^{-1}, $S_{2,m}$ the strength of the corresponding transition and $g_{2,m}$ the degeneracy of the excited level

m	$\Delta_{2,m}$ [cm^{-1}]	$g_{2,m}$	$g_{2,m}\cdot S_{2,m}$
mixed dimer, $n=2$			
1	−24.7±0.5	1	1.84
2	7.5±0.3	1	0.16
3	−19.6±0.3	2	0.76
4	2.4±0.1	2	3.24

Following the assumption that the SF_6-molecule behaves like an isotropic oscillator, the influence of the rotational states is entirely neglected.

In Table 2 the energy shifts $\Delta_{n,m}$, in units of $(4\pi\varepsilon_0)^{-1}\cdot\mu_{01}^2\cdot\langle R^{-3}\rangle$, are shown. In our case the fundamental frequency of the ν_3-mode is 948 cm^{-1} [8] and the transition dipole moment $\mu_{01}=0.388D$ [5]. One has to take as unit the value of (6.8 ±0.2) cm^{-1} in order to be consistent with the experimental data for the dimer and the trimer, as will be discussed below. In Table 2 also is shown the transition strength $S_{n,m}$ for a vibrational transition of a cluster, relative to the transition strength of a monomer $S_{1,1}$. The sum over all the products of transition strengths $S_{n,m}$ and degeneracy $g_{n,m}$ of an n-cluster is $3n$, in accordance with the sum rule.

In the SF_6-beam there is a natural abundance of 4% of the $^{34}SF_6$-isotope; its ν_3-frequency is red shifted by 17 cm^{-1} [8] with respect to the main $^{32}SF_6$-component. Therefore, we expect also to find an attenuation signal caused by predissociation of the mixed-dimer $^{34}SF_6\cdot{}^{32}SF_6$, on mass $^{34}SF_5^+$ as well as on mass $^{32}SF_5^+$, if the correct laser lines are chosen. The mixed dimer possesses three times two nearly degenerate states (17 cm^{-1} apart) which have off-diagonal elements due to the dipole-dipole interaction of +6.8 cm^{-1} and −13.6 cm^{-1}, depending on whether the dipole moments are perpendicular or parallel to the intermolecular axis. In Table 3 the energy shifts $\Delta_{n,m}$ and the transition strengths $S_{n,m}$ for the mixed-dimer are displayed. In Fig. 2 the stick-spectra for $(^{32}SF_6)_n$, $n=1,\text{--},6$, and for the mixed-dimer $^{34}SF_6\cdot{}^{32}SF_6$ are shown.

4. The Fit Procedure

Above we have calculated the theoretical spectrum, for a dominant dipole-dipole interaction. In order to compare these results to our measurements we must assume a certain line form and line width, for the different cluster-transitions. A Lorentz-profile has been chosen without, however, implying that the line

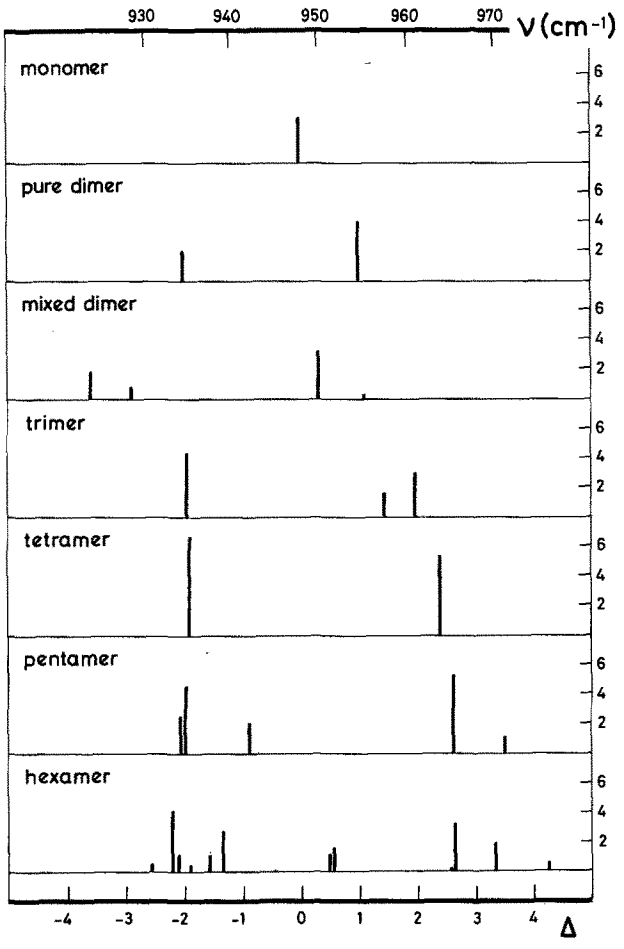

Fig. 2. The stick spectrum. The energy shift Δ is given below in units of $(4\pi\varepsilon_0)^{-1}\cdot\mu_{01}^2\cdot\langle R^{-3}\rangle$. On the upper scale use is made of the fit to the experimental dimer results. The relative intensity corresponds to $g\cdot S$, see Tables 2 and 3

width is necessarily caused by predissociation lifetime.

We propose a very simple model to explain the dissociation of the clusters; rapid predissociation of the excited cluster supersedes stimulated emission. The probability of dissociation d_n of N_n n-clusters is

$$d_n = N_n\cdot\exp(-r_n\cdot t) \tag{4.1}$$

where t is the laser interaction time and r_n is the rate of excitation of a n-cluster. The difference of the mass spectrometer signal without and with laser action contains the factor $(1-\exp(-r_n\cdot t))$. Normally, the mass spectrometer signal is determined not only by the concentration of n-clusters, but also by their relative ionization and fragmentation probability upon electron bombardment. We take the ionization probability proportional to n; the monomer ionization probability equals α_1. The fragmentation probability of a cluster of size n to an ion of size k – i.e. $SF_5^+\cdot(SF_6)_{k-1}$ – is denoted by f_{kn}. The observed difference of the ion signal, without and with laser, amounts to

$$\Delta I_k = \alpha_1\cdot\sum_{n\geqq k} n f_{kn} N_n (1-\exp(-r_n\cdot t)) \tag{4.2}$$

The product of the rate r_n and the interaction time t can be written as

$$r_n\cdot t = \sum_m \frac{\mu_{01}^2}{\hbar^2\varepsilon_0}\cdot\frac{F}{c}\cdot\frac{2}{\Gamma_{n,m}}\cdot\frac{g_{n,m}\cdot S_{n,m}}{3}\cdot\frac{(\Gamma_{n,m}/2)^2}{(\omega-\omega_{n,m})^2+(\Gamma_{n,m}/2)^2} \tag{4.3}$$

where F represents the laser fluency and μ_{01} the transition dipole moment; $\omega_{m,n}$, $\Gamma_{m,n}$, $g_{n,m}$ and $S_{n,m}$ stand for the (angular) transition frequency, the line width, the degeneracy and the strength of a particular transition m of an n-cluster. The degeneracy and strength of a transition are shown in Table 2. The transition frequency can be taken from the same table, $\hbar\omega_{m,n} = 948\,\mathrm{cm}^{-1} + \Delta_{m,n}$, where a scaling was already applied by fitting the experimental results – one unit corresponds with $(6.8\pm0.2)\,\mathrm{cm}^{-1}$ –; the line width has to be fitted, too, from the experimental results. Writing down (4.3) a Lorentz-profile was assumed to describe the experiments.

Our He-seeded SF_6 beams allowed the observations of dimers and trimers, only, i.e. $n\leqq 3$, in accordance with the absence of any trace of $SF_5^+\cdot(SF_6)_3$ in our mass spectra, see Fig. 3. In Figs. 4–7 the experimental results – obtained on the ion-mass SF_5^+ with 1 W laser power – are displayed together with the fit using (4.2). The calculated rate r_2 has been tested at a frequency of $935\,\mathrm{cm}^{-1}$ and a stagnation pressure $P_0 = 1{,}000$ torr where only monomers and dimers are present in the beam in a measurable amount. The product $r_2\cdot t = 0.36$ is calculated for a molecular beam velocity of 870 m/s, a laser waist of 0.7 mm at the point of intersection, $\Gamma_2 = \Gamma_{2,1} = \Gamma_{2,3} = 1.5\,\mathrm{cm}^{-1}$ and for 1 W laser power. The power dependence of the attenuation signal at $P_0 = 1{,}000$ torr does not allow a very precise determination of $r_2\cdot t$; $r_2(1\,\mathrm{W})\cdot t = 0.36$ describes the observation very well (Fig. 8). An uncertainty of 30% in the rate r_2 yields a 10% variation of ΔI_∞, the attenuation at high laser fluency. – In parenthesis, $r_2(1\,\mathrm{W})\cdot t = 0.36$ corresponds to a photodissociation cross section of $0.5\cdot10^{-20}\,\mathrm{m}^2$, for the red dimer peak at $935\,\mathrm{cm}^{-1}$.

5. The Fragmentation Probabilities

From our measurements quantitative conclusions can be drawn with respect to the fragmentation

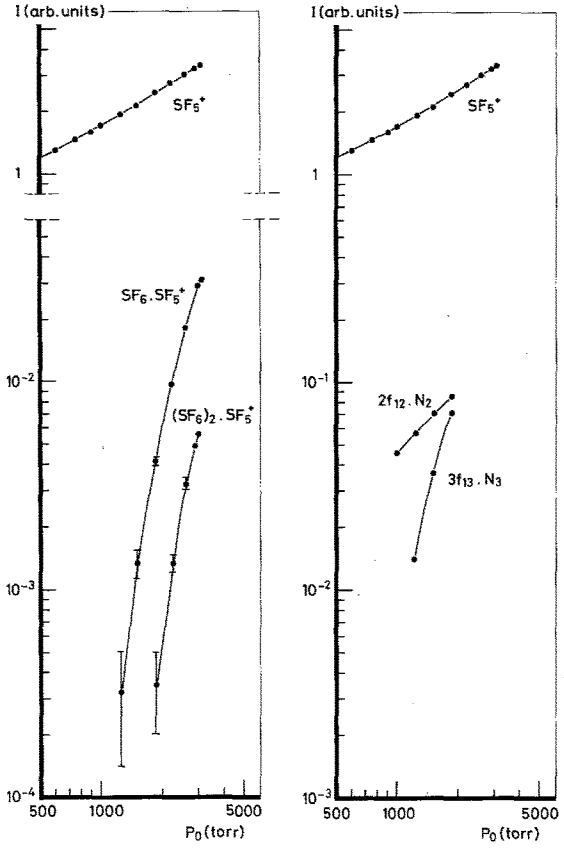

Fig. 3. Mass spectrometric (left) and spectropic (right) intensities vs. the stagnation pressure P_0. The SF_5^+-signal corresponds to the mass spectrometric signal of the SF_6-beam; at higher stagnation pressures this signal contains cluster-admixtures to a maximum of 4%. The $SF_6 \cdot SF_5^+$ $[(SF_6)_2 \cdot SF_5^+]$-signal normally is taken as a measure of dimer [trimer]-concentrations. The $2f_{12} \cdot N_2[3f_{13}N_3]$-signal is more than ten times stronger and correspond to the actual cluster intensity; $f_{12} \geqq 0.99$ $[f_{13} \geqq 0.93]$ at $P_0 = 1850$ torr (see Sect. 5). The spectroscopic signals are the saturated values (e.g. $2f_{12}N_2$) for high laser power

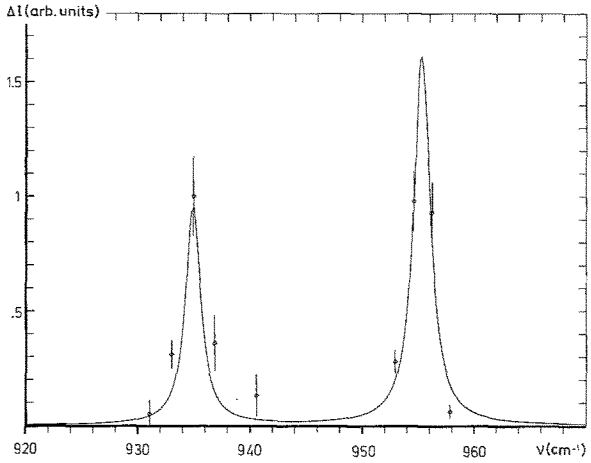

Fig. 4. The cluster spectrum, at $P_0 = 1{,}000$ torr, $T_0 = 233$ K and 1 W laser power. The fit (solid curve) yields $\Gamma_2 = 1.5 \pm 0.4\,cm^{-1}$, $2f_{12}N_2/(f_{11}N_1 + 2f_{12}N_2 + 3f_{13}N_3) = (2.7 \pm 0.5)$ and $3f_{13}N_3/(f_{11}N_1 + 2f_{12}N_2 + 3f_{13}N_3) =$ zero. Optimum agreement was found for $(4\pi\varepsilon_0)^{-1}\mu_{01}^2\langle R^{-3}\rangle = 6.8\,cm^{-1}$. The unshifted frequency was taken equal to $948.5\,cm^{-1}$. The spectrum is normalized (see *NF*, Table 4)

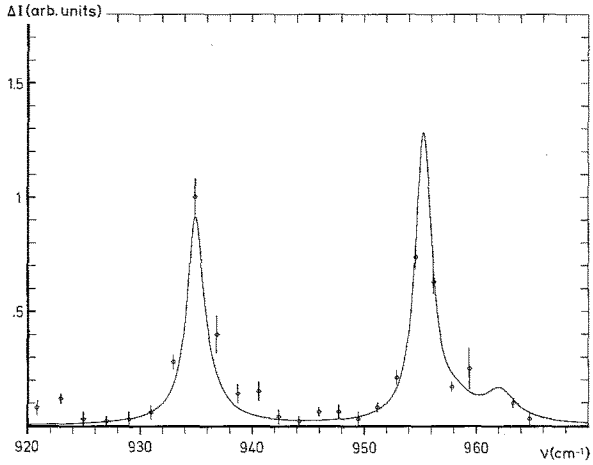

Fig. 5. The cluster spectrum, at $P_0 = 1{,}250$ torr. The fit (solid curve) with fixed $\Gamma_2 = 1.5\,cm^{-1}$ (see Fig. 4) and with fixed $\Gamma_3 = 3.3\,cm^{-1}$ (see Fig. 6) yields $2f_{12}N_2/(f_{11}N_1 + 2f_{12}N_2 + 3f_{13}N_3) = (3.0 \pm 0.4)\%$ and $3f_{13}N_3/(f_{11}N_1 + 2f_{12}N_2 + 3f_{13}N_3) = (0.8 \pm 0.2)\%$. Further details in caption of Fig. 4

probabilities f_{kn}. First the reminder that $k = 1(2)$ stands for the probability that an n-cluster fragments to SF_5^+ $(SF_5^+ \cdot SF_6)$; a fragmentation to masses like SF_3^+ or $SF_3^+ \cdot SF_6$ was not systematically studied in the present work, though roughly speaking a repetition of the relative monomer-fragment-intensities SF_x^+ for $1 \leqq x \leqq 5$ was observed amongst the $SF_6 \cdot SF_x^+$ fragments.

The value of $nf_{1n}N_n$ can be obtained from the fit displayed in Figs. 4–7. In the corresponding captions the ratios $nf_{1n}N_n/(\sum_{\nu=1} \nu f_{1\nu}N_\nu)$ are given which multiplied by the strength of the SF_5^+-signal yield $2f_{12}N_2$ and $3f_{13}N_3$.

From Fig. 3 one learns that $f_{12}/f_{22} \geqq 100$, at $P_0 = 1{,}250$ torr; this follows directly from the ratio R of the $2f_{12}N_2$-signal to the $SF_5^+ \cdot SF_6$ signal, the latter one being ideally equal to $2\alpha_1 f_{22}N_2$. This ratio assumes the value 100 if admixture from larger clusters is neglected to the $SF_5^+ \cdot SF_6$-signal. For higher P_0-values the ratio R assumes smaller values; yet the highest masured value $f_{12}/f_{22} = 100$ should hold for f_{12}/f_{22}, also at these higher pressures, as lower limit; e.g. $R = 20$ at $P_0 = 1{,}850$ torr evidently points to the influence of trimers contributing to the $SF_5^+ \cdot SF_6$-signal.

Next we use the plausible assumption that the total ionization probability that an n-cluster yields an ion cluster containing SF_5^+ equals the monomer frag-

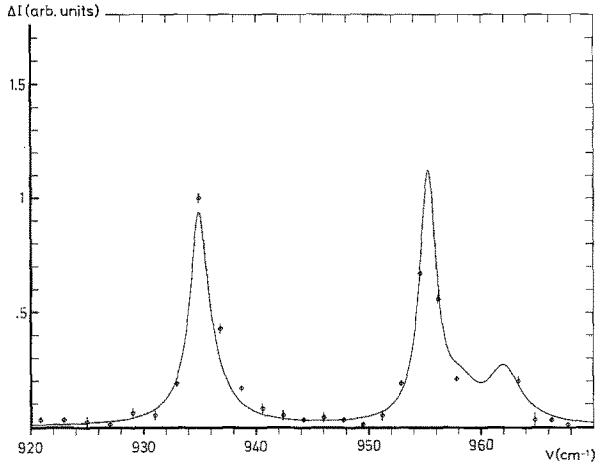

Fig. 6. The cluster spectrum at $P_0=1{,}500$ torr. With fixed $\Gamma_2=1.5\,cm^{-1}$ the fit yields $2N_2f_{12}/(f_{11}N_1+2f_{12}N_2+3f_{13}N_3)=(3.5\pm0.5)\,\%$ and $3N_3f_{13}/(f_{11}N_1+2f_{12}N_2+3f_{13}N_3)=(1.8\pm0.3)\,\%$. The line width for this P_0-value was determined to $\Gamma_3=(3.3\pm0.4)\,cm^{-1}$ considering, too, measurements at 0.5 W and 2.5 W. Further details in the caption of Fig. 4

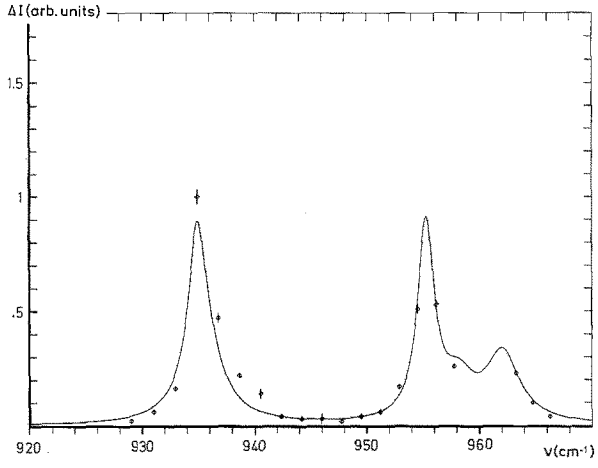

Fig. 7. The cluster spectrum at 1,850 torr. With fixed $\Gamma_2=1.5\,cm^{-1}$ and $\Gamma_3=3.3\,cm^{-1}$ the fit yields $2f_{12}N_2/(f_{11}N_1+2f_{12}N_2+3f_{13}N_3+4f_{14}N_4)=(3.6\pm0.6)\,\%$ and $3f_{13}N_3/(f_{11}N_1+2f_{12}N_2+3f_{13}N_3+4f_{14}N_4)=(3.0\pm0.5)\,\%$ and $4f_{14}N_4/(f_{11}N_1+2f_{12}N_2+3f_{13}N_3+4f_{13}N_4)=$ zero. The trimer shoulder at $962\,cm^{-1}$ is clearly visible. Further details in the caption of Fig. 4

mentation probability f_{11} to SF_5^+, i.e.

$$f_{11}=\sum_{k=1}^{n} f_{kn}. \tag{5.1}$$

The violent eruption of SF_6^+ emitting an uncharged F-atom is not measurably influenced by the presence of loosely bound SF_6-partners, an assumption plausible at least for small n-values.

Then, $f_{12}/f_{22}\geqq 100$ yields $0.99\leqq f_{12}/f_{11}\leqq 1$. Hence, one can simplify the fit-parameter of caption 4, $2f_{12}N_2/(f_{11}N_1+2f_{12}N_2)\approx 2N_2/(N_1+2N_2)$ within 1 % (see Table 4).

For $P_0=1{,}850$ torr, the ratio of the $3f_{13}N_3$ - to the $SF_5^+\cdot(SF_6)_2$ - signal yields $f_{13}/f_{33}\geqq 150$, the inequality again because of possible contributions of larger clusters to the latter signal. Similarly, the ratio of the $3f_{13}N_3$ - to the $SF_5^+\cdot SF_6$-signal yields $f_{13}/f_{23}\geqq 15$; here the inequality stems from possible contributions of larger and smaller (i.e. dimer) clus-

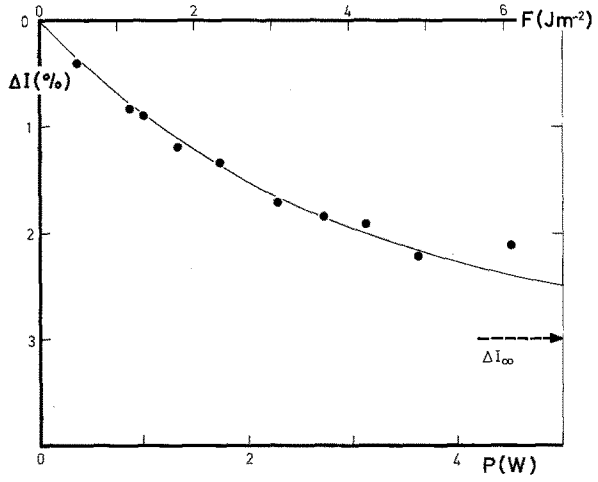

Fig. 8. Beam attenuation vs. laser power, at $935\,cm^{-1}$. Measurements were performed at $P_0=1{,}000$ torr (see Fig. 4). The upper scale, F, indicates the laser fluency, seen by the dimers. The experimental results (•) have been compared to a $(1-\exp(-r_2\cdot t))$-dependence with $r_2(1\,W)\cdot t=0.36$ (solid curve). $\Delta I_\infty=(3.0\pm0.1)\,\%$ means that 1.5 % dimers are present in the beam

Table 4. Cluster concentrations for different stagnation pressures P_0. The second column (NF) yields the normalization factor leading from the normalized spectra in Figs. 4–7 to the observed beam attenuations. The third and fourth column describe the dimer and trimer concentrations, N_2/N_1 and N_3/N_1, obtained from the fits to the spectra in Figs. 4–7. The uncertainty corresponds to one standard deviation. The fifth column yields the relative number of SF_6 molecules bound in dimers and trimers (the sum of column 3 and 4). This can be compared to the last column, obtained from the saturation behaviour, e.g. displayed in Fig. 8

P_0 [torr]	$10^{-2}\cdot NF$	$2N_2/N_1$ %	$3N_3/N_1$ %	$(2N_2+3N_3)/N_1$ %	$(2N_2+3N_3)/N_1$ %
1,000	0.86 ± 0.09	2.7 ± 0.5	–	2.7 ± 0.5	3.0 ± 0.1
1,250	1.23 ± 0.12	3.0 ± 0.5	0.8 ± 0.2	3.8 ± 0.7	–
1,500	1.65 ± 0.17	3.5 ± 0.5	1.8 ± 0.3	5.3 ± 0.8	4.8 ± 0.2
1.850	2.16 ± 0.22	3.6 ± 0.6	3.0 ± 0.5	6.6 ± 1.1	6.7 ± 0.2

ters to the $SF_5^+ \cdot SF_6$-signal. Assumption (5.1) then gives $0.93 \leqq f_{13}/f_{11} \leqq 1$. Again one can simplify the fit parameter of Fig. 5,

$$3f_{13}N_3/(f_{11}N_1+2f_{12}N_2+3f_{13}N_3) \approx 3N_3/(N_1+2N_2+3N_3),$$

within 8% (see Table 4).

6. Discussion

It should be clear from the foregoing that we do not pretend to have achieved high resolution spectroscopy of SF_6-clusters, neither experimentally nor what concerns the theoretical treatment. On the other hand spectra have been obtained at probing frequencies spaced by about $2\,cm^{-1}$ which show a remarkable structure; a very simple theoretical model seems to explain very well this observed structure with a single parameter, i.e. $(4\pi\varepsilon_0)^{-1} \cdot \mu_{01}^2 \cdot \langle R^{-3} \rangle = 6.8\,cm^{-1}$.

The Lorentzian line widths $\Gamma_{n,m}$ introduced to reproduce the line shape perhaps suggests that the lifetime of the vibrationally excited clusters is of dominant influence on the line widths. In our opinion, however, there is no evidence for such interpretation; it is equally possible that the width reflects the internal state distribution of the excited cluster.

We have assumed, in our fits displayed in Figs. 4–7, that $\Gamma_{n,m}$ is independent of the level index m (see Table 2). Inspection of Fig. 4 demonstrates that this assumption can be questioned; the $(n,m)=(2,1)$ peak seems clearly broader than the (2, 3) peak. In view of the coarse nature of our results we felt an introduction of different width $\Gamma_{n,m}$ for the different transitions m of one n-cluster unwarranted.

The fact that for the trimer we had to apply a two times larger $\Gamma_3(3.3 \pm 0.4\,cm^{-1})$ as compared to $\Gamma_2(1.5 \pm 0.4)$ may point to a shorter lifetime as well as to the lifting of the degeneracy of the more numerous internal states (e.g. van der Waals stretching modi). This energy splitting can be influenced by hexadecapole forces or angle dependent dispersion forces.

The mixed dimer $^{32}SF_6 \cdot {}^{34}SF_6$ shows experimentally a transition at $921 \pm 2\,cm^{-1}$ compatible with the theoretical value $923\,cm^{-1}$. One deduces $\mu_{01}(^{32}S) \cdot \langle R^{-3}(^{32}S - {}^{32}S) \rangle / \mu_{01}(^{34}S) \cdot \langle R^{-3}(^{34}S - {}^{32}S) \rangle = 0.9 \pm 1$. Due to the natural abundance, the mixed dimer peak is expected to be about a factor 25 weaker than the pure dimer peak ($935\,cm^{-1}$), a ratio born out by the experiment (Fig. 9).

Table 4 displays absolute concentrations of clusters in the SF_6 beam determined by our fit procedure.

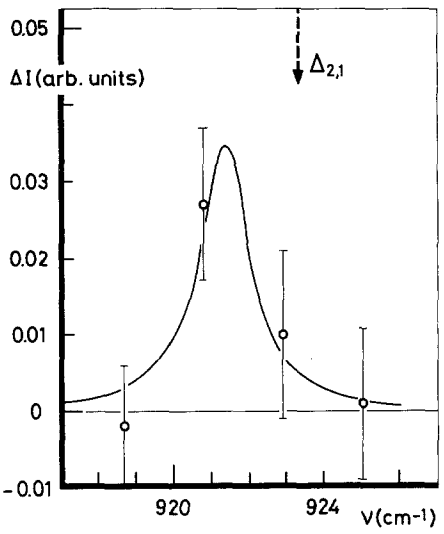

Fig. 9. A $^{32}SF_6 \cdot {}^{34}SF_6$ dimer line. Detail study of Fig. 6 around $923\,cm^{-1}$ (dashed arrow) where the stick spectrum predicts a mixed dimer transition. The contribution of pure $^{32}SF_6$-clusters has been subtracted, utilizing the fitted spectrum of Fig. 6. The solid line corresponds to a fitted Lorentzian (with $\Gamma_2 = 1.5\,cm^{-1}$) centered at $\Delta_{2,1} = (-26.5 \pm 1.5\,cm^{-1})$

(For a consistency check, the concentrations were, too, determined from the saturation behaviour of the attenuation at a fixed frequency ($935\,cm^{-1}$) and found in good agreement). Compared to the large uncertainties of purely mass spectrometric cluster detection due to fragmentation processes in the ionizer our rather precise spectroscopic determination contrasts satisfactorily. Figure 3 allows to compare directly the spectroscopic determination of the dimer and trimer concentration (at right) to the conventional mass spectrometer signals (at left). The two determinations differ by more than a factor ten.

In addition, the fragmentation can be directly measured by measuring the attenuation signal at fixed laser frequency for different masses [1].

Preliminary experiments at an electron energy of 25 eV indicate that fragmentation may be significantly reduced; we shall investigate this suggestion [11] in the future. – A second extension of the current investigation will employ two lasers; a chopped one to mark a cluster signal setting the frequency to a clear spectral peak, the other to scan the entire spectrum. Thereby we expect to resolve the spectrum of larger clusters, for fixed sizes.

After completion of this work we became acquainted with two recent important papers on similar objects. Casassa et al. [13] have thoroughly investigated the system C_2H_4, Van der Waals bonded to C_2H_4, C_2F_4, Ne, Ar and Kr. Lisy et al. [14] have found the ring structure of $(HF)_n$, $n=3$ to 6, from the predissociation spectra.

This work is part of the research program of the "Stichting Fundamenteel Onderzoek der Materie (F.O.M.)" and has been made possible by financial support from the "Nederlandse Stichting voor Zuiver-Wetenschappelijk Onderzoek (Z.W.O.)".
We thank F. Lapoutre for his valuable assistance.

References

1. Geraedts, J., Setiadi, S., Stolte, S., Reuss, J.: Chem. Phys. Lett. **78**, 277 (1981)
2. Mulliken, R.S.: Phys. Rev. **120**, 1674 (1960)
3. Hirschfelder, J., Curtis, C., Bird, R.: Molecular Theory of gases and liquids. p. 992. New York: Wiley & Sons 1965
4. Margenau, H., Kestner, N.: Theory of intermolecular forces. 2nd ed., p. 291. Oxford: Pergamon Press 1971
5. Fox, K., Person, W.: J. Chem. Phys. **64**, 5218 (1976)
6. Morales, D., Ewing, G.: Chem. Phys. **53**, 141 (1980)
7. Gough, T., Miller, K., Scoles, G.: J. Chem. Phys. **69**, 1588 (1978)
8. Brodbeck, C., Rossi, I., Strapelias, H., Bouanic, J.P.: Chem. Phys. **54**, 1 (1980)
9. The nozzle is a cheap Pt–Ir lens fabricated for an electronmicroscope (Siemens or Philips). It is soft-soldered to a stainless-steel pipe (3 mm ∅). This pipe is enclosed by a copper block, cooled by contact with a liquid nitrogen reservoir and stabilized by the energy dissipation of a transistor. The temperature of the block can be controlled from 100 to 300 K
10. The help of Dr. H. Bluyssen and A. van Etteger who provided us with their well fuctioning CO_2 laser and many advices is gratefully acknowledged
11. Bonissent, A., Mutaftschiev, B.: J. Chem. Phys. **58**, 3727 (1973)
12. Echt, O., Sattler, K.: Private communication (1981)
13. Casassa, M.P., Bomse, D.S., Janda, K.C.: J. Chem. Phys. **74**, 5044 (1981)
14. Lisy, J.M., Tramer, A., Vernon, M.F., Lee, Y.T.: J. Chem. Phys. (to be published)

J. Geraedts
S. Stolte
J. Reuss
Fysisch Laboratorium
Katholieke Universiteit
NL-6525 ED Nijmegen
The Netherlands